Published in final edited form as:
J Neurochem. 2013 March ; 124(6): . doi:10.1111/jnc.12139.

Striatal CB_1 and D_2 receptors regulate expression of each other, CRIP1A and delta opioid systems

Lawrence C. Blume[*], **Caroline E. Bass**[*,1], **Steven R. Childers**[*], **George D. Dalton**[*], **David C. S. Roberts**[*], **Jasmine M. Richardson**[*,1], **Ruoyu Xiao**[*], **Dana E. Selley**[†], and **Allyn C. Howlett**[*]

[*]Department of Physiology and Pharmacology, Wake Forest University Health Sciences, Winston-Salem, North Carolina, USA

[†]Department of Pharmacology and Toxicology, Virginia Commonwealth University, Richmond, Virginia, USA

Abstract

Although biochemical and physiological evidence suggests a strong interaction between striatal CB_1 cannabinoid (CB_1R) and D_2 dopamine (D_2R) receptors, the mechanisms are poorly understood. We targeted medium spiny neurons of the indirect pathway using shRNA to knockdown either CB_1R or D_2R. Chronic reduction in either receptor resulted in deficits in gene and protein expression for the alternative receptor and concomitantly increased expression of the cannabinoid receptor interacting protein 1a (CRIP1a), suggesting a novel role for CRIP1a in dopaminergic systems. Both CB_1R and D_2R knockdown reduced striatal dopaminergic-stimulated [^{35}S] GTPγS binding, and D_2R knockdown reduced pallidal WIN55212-2-stimulated [^{35}S]GTPγS binding. Decreased D_2R and CB_1R activity was associated with decreased striatal phosphoERK. A decrease in mRNA for opioid peptide precursors pDYN and pENK accompanied knockdown of CB_1Rs or D_2Rs, and over-expression of CRIP1a. Down-regulation in opioid peptide mRNAs was followed in time by increased DOR1 but not MOR1 expression, leading to increased [D-Pen2, D-Pen5]-enkephalin-stimulated [^{35}S]GTPγS binding in the striatum. We conclude that mechanisms intrinsic to striatal medium spiny neurons or extrinsic via the indirect pathway adjust for changes in CB_1R or D_2R levels by modifying the expression and signaling capabilities of the alternative receptor as well as CRIP1a and the DELTA opioid system.

Keywords

basal ganglia; cannabinoid receptor; enkephalin; gene expression; medium spiny neurons; mesolimbic dopamine pathway

Compelling behavioral, anatomical, and physiological evidence suggests a strong relationship between cannabinoid and dopamine systems, especially between CB_1 cannabinoid receptors (CB_1R) and D_2 dopamine receptors (D_2R) (reviewed in (Fernandez-Ruiz *et al.* 2010; Smith and Villalba 2008). Both CB_1Rs and D_2Rs are G protein-coupled

Address correspondence and reprint requests to: Allyn C. Howlett, Department of Physiology and Pharmacology, Wake Forest University Health Sciences, One Medical Center Blvd., Winston-Salem, NC 27157 USA. ahowlett@wakehealth.edu.
[1]Present address: CEB: Department of Pharmacology and Toxicology, University at Buffalo, Buffalo, NY 14214 USA; JMR: College of Pharmacy and Health Sciences, Campbell University, Buies Creek, NC 27506 USA.

The authors have no conflicts of interest to declare.

Supporting information
Additional supporting information may be found in the online version of this article at the publisher's website.

receptors highly expressed in the striatum, and are key proteins in the processing of basal ganglia neurotransmission (Sanudo-Pena *et al.* 1999; van der Stelt and DiMarzo 2003; Fernandez-Ruiz 2009; Lovinger 2010). CB_1Rs and D_2Rs have been found to be co-localized in the enkephalin-containing medium spiny neurons (MSN) of the striatum, as well as being co-expressed on the axon terminals at the globus pallidus (indirect striatopallidal pathway) (Gerfen *et al.* 1990; Mailleux and Vanderhaeghen 1992; Szabo *et al.* 1998; Hermann *et al.* 2002; Matyas *et al.* 2006; Crespo *et al.* 2008; Martin *et al.* 2008; Van Waes *et al.* 2012). In addition, CB_1Rs and D_2Rs are observed in close proximity on soma and dendritic spines of neurons within the ventral striatum (Pickel *et al.* 2006). The close alignment of these two receptors within protein complexes has been substantiated with fluorescence resonance energy transfer or multicolor bimolecular fluorescence complementation studies in heterologous expression systems (Marcellino *et al.* 2008; Przybyla and Watts 2010).

In support of their close anatomical co-localization, functional interactions from biochemical data identified that CB_1Rs and D_2Rs converge to share Gi/o proteins or adenylyl cyclase effectors in striatal membranes (Meschler and Howlett 2001). Other studies identified a switch in the G protein coupling resulting in an increase in cAMP production upon simultaneous treatment by both CB_1R and D_2R agonists in cultured neonatal striatal cells (Glass and Felder 1997) or by co-expression of both CB_1Rs and D_2Rs in host cells (Jarrahian *et al.* 2004; Kearn *et al.* 2005). However, to date, a direct functional relationship between CB_1Rs and D_2Rs in MSNs of the basal ganglia has not clearly been established, and as such remains poorly understood.

On the basis of these data, we hypothesize that CB_1Rs and D_2Rs can interact in striatal neurons to cooperatively regulate cellular function in the basal ganglia *in vivo*. To determine how one receptor influences the cellular signaling by the other receptor, we used RNA interference to suppress the synthesis of either CB_1Rs or D_2Rs in rat dorsal striatum. Here, we present data demonstrating a physiologically relevant coupling of CB_1R and D_2R regulation at the transcript, protein and signaling level in rat basal ganglia circuitry. These results reveal a pattern of functional mimicry for these two G protein-coupled receptors associated with homeostatic adaptations in basal ganglia signaling. These studies also uniquely identify a contribution of the CRIP1a protein to cellular regulation of signaling by both CB_1Rs and D_2Rs *in vivo*. CRIP1a is an accessory protein that has been shown to regulate CB_1R-mediated tonic inhibition of voltage-dependent Ca^{2+} channels (Niehaus *et al.* 2007), presumably at the pre-synaptic terminals. The present data suggest that CRIP1a is important in regulating signal transduction in the striatopallidal pathway.

Material and methods

Materials

WIN55212 was purchased from Tocris, and *N*-propylnorapomorphine (NPA), [D-Ala2, NMe-Phe4, Gly-ol5]-enkephalin (DAMGO) and [D-Pen2, D-Pen5]-enkephalin (DPDPE) were purchased from Sigma, St Louis, MO, USA. [^{35}S]GTPγS was purchased from PerkinElmer, Waltham, MA, USA. Dulbecco's Modified Eagle's Medium was purchased from Gibco Life Technologies (Gibco, Rockville, MD, USA). All other chemicals were reagent grade and purchased from Sigma-Aldrich or specialized suppliers as indicated.

Cloning of adeno-associated viral plasmids and generation of viruses

For viruses designed for RNA interference-directed knockdown of the expression of CB_1Rs and D_2Rs, oligos encoding short hairpin RNA (shRNA) sequences were cloned into an adeno-associated viral (AAV) plasmid, EGFP-U6-pACP, described previously (Sadri-Vakili *et al.* 2010). In this plasmid, the cytomegalovirus promoter drives expression of the

enhanced green fluorescent protein (EGFP) gene, which is cloned with an intron/polyA sequence derived from SV40. shRNA expression is driven by a murine U6 pol III promoter which is located downstream of the EGFP cassette. The entire EGFP and U6 transgenes are flanked by AAV2 inverted terminal repeats. Each of the synthetic oligos, encoding the shRNA and its respective complement (Sigma-Aldrich), were annealed and ligated into unique *BbsI* and *NheI* sites after the U6 promoter. The target sequences were selected by the siRNA target finder program on the GenScript website (https://www.genscript.com/ssl-bin/app/rnai) using the mRNA sequences NM_012784 (rat Cnr1 mRNA) and NM_012547 (rat Drd2 mRNA). Three different AAV-shCB_1R and AAV-shD_2R viruses were created, and each was individually tested for knockdown efficiency. A control vector consisted of an identical EGFP transgene but encoded a scrambled shRNA that does not correspond to any known rat mRNA sequence (determined from a BLAST search).

For the virus designed to over-express mouse CRIP1a, total mRNA from mouse cortex was isolated and converted to cDNA using a High-Capacity cDNA Archive Kit (Applied Biosystems, Foster City, CA, USA), and CRIP1a cDNA was amplified by reverse transcriptase polymerase chain reaction (PCR). The forward primer 5′-aatttctagaGCCACCATGGGGGACCTACCC-3′ and the reverse primer 5′-ggccaagcttTCAGAGGAAGGACTCCTTATT-CACCCA-3′ provided an *Xba*I restriction site upstream of the translation initiation codon, a Kozak sequence and a *Hind*III site downstream of the translation stop codon of the CRIP1a fragment. The 0.5 kb PCR product was verified by sequence analysis, and subcloned into pACP at the *Xba*I and *Hind*III sites. This plasmid (CRIP1a-pACP) consists of two AAV2 inverted terminal repeats flanking the cytomegalovirus promoter, CRIP1a cDNA, and an intron and polyadenylation signal sequence derived from SV40.

Packaging of all recombinant AAVs was carried out according to a standard triple transfection protocol to create pseudotyped AAV2/ 10 virus (Xiao *et al.* 1998). The AAV2/10 rep/cap plasmid provides the AAV2 replicase and AAV10 capsid genes (Gao *et al.* 2002; De *et al.* 2006), and adenoviral helper functions were provided by the pHelper plasmid (Stratagene). AAV-293 cells were transfected with 10 μg of pHelper and 1.15 pmol each of AAV2/10 and AAV vector plasmids to be used in this study. The cells were harvested 48 h later, and clarified viral lysates were isolated from the cell pellets. The virus was pooled, aliquoted, and stored at −80°C. AAV-vector stocks were titered by real-time quantitative PCR (qPCR) (Eppendorf Realplex) using primers and probe sets designed to amplify a sequence in the SV40 intron.

Stereotaxic intracranial injections of AAV-viruses

Adult male Sprague–Dawley rats weighing 280–310 g (Harlan Inc., Indianapolis, IN, USA) were used, and experimental procedures were approved by the Wake Forest University Institutional Animal Care and Use Committee and followed the ARRIVE guidelines (Kilkenny *et al.* 2010). Prior to surgery, animals were anesthetized with a combination of ketamine (100 mg/kg) and xylazine (8 mg/ kg, i.p.). Rats were placed into a stereotaxic frame (Kopf), 1 mm holes were drilled into the skull, and a 10 μL Hamilton syringe fitted within a 30 gauge needle was used for viral delivery. All injections were made into the dorsal striatum using the following coordinates relative to bregma, with the tooth bar set to + 0.5 mm: anteroposterior (AP): + 0.5 mm, mediolateral (ML): ± 2.8 mm, dorsoventral (DV): + 4.4 mm relative to stereotaxic zero (Paxinos and Watson 1997) (see Figure S2). AAV-scramble, a mixture of three AAV-shCB_1R, a mixture of three AAV-shD_2R, or AAV-CRIP1a (4 μL) were unilaterally injected at a rate of 0.5 μL/min. To reduce back-flow of viral solution, the needle remained in place ten min post-injection before being slowly removed. To avoid issues of lateralization, injections of AAV were made in either the left or right hemispheres with equal frequency within each experimental group of rats. Animals

were sutured, and revived on a heating pad before being returned to their home cages (two animals per cage).

Analysis of gene expression in AAV-injected brains

Rats were killed at 3, 5, 10, 17, 21, 30, or 56 days post-injection of AAV, and brains were dissected and placed in an ice cold brain matrix. Coronal brain slices (2 mm) were taken at the site of injection, placed on a chilled dissecting block, and 2 mm-diameter circular brain punches were collected ipsilaterally (treated) and contralaterally (control). Total RNA was isolated and purified using an RNeasy Mini Kit (Qiagen, Valencia, CA, USA). Total RNA (1 μg) was reverse transcribed into cDNA using a High-Capacity cDNA Archive Kit (Applied Biosystems, Foster City, CA, USA). Real-time qPCR was performed using TaqMan Universal PCR Master Mix and specific TaqMan primer-probe MGB assay sets (Applied Biosystems) for the following genes: 18s ribosomal RNA, neuron-specific enolase 2 (eno2), CB_1 cannabinoid receptor (cnr1), CRIP1a (cnrip1), delta opioid receptor (Oprd1), D_2 dopamine receptor (drd2), mu opioid receptor (Oprm1), pro-enkephalin (PENK), pro-dynorphin (PDYN). Data were analyzed using the ΔΔCT method comparing the ipsilateral to the contralateral side (Gerald *et al.* 2006), and eno2 on the side contralateral to the injection served as the reference standard.

Generation of CRIP1a antibody

We generated a rabbit polyclonal antibody against rat CRIP1a corresponding to amino acids D20-F32 (AbD20) (Figure S2a). The peptide was synthesized and conjugated by disulfide formation with keyhole limpet hemocyanine, rabbit antibodies generated and affinity-purified, and titered using an ELISA (GenScript, Piscataway, NJ, USA). To verify avidity and specificity for CRIP1a, we compared this novel antibody with a previously characterized CRIP1a antibody, CRIP1a AbK148, which recognizes the last 17 amino acids of CRIP1a (K148-L164) (Elphick *et al.* 2004; Niehaus *et al.* 2007). Western blot analyses of striatal crude homogenates identified a band at the same mobility at various antibody dilution factors (1 : 50, 1 : 100, 1 : 300, 1 : 1000) using either CRIP1a AbD20 or AbK148 (data not shown).

Immunohistochemistry of protein levels in brain slices

Effects of shCB_1R and shD_2R knockdown, and CRIP1a over-expression on total protein levels of CB_1R, CRIP1a, D_1R, DOR1, MOR1, cAMP-response element binding protein (CREB), phospho-CREB, ERK, and phospho-ERK were quantitated using a modified immunohistochemistry technique (Kearn 2004). Anesthetized animals were decapitated, brains were dissected, snap-frozen in isopentane cooled by dry ice, and stored at −80°C. Frozen brains were sectioned at 40 μm using a cryostat microtome, slices were placed into a 24-well plate containing frozen phosphate-buffered formalin (1.5 mM KH_2PO_4, 2.7 mM KCl, 8 mM Na_2HPO_4, 150 mM NaCl; 30% sucrose (w/v); 3% paraformaldehyde (v/v), pH 7.4), and stored at 4°C. Slices were washed in Tris-buffered saline (TBS) (20 mM Tris-HCl, pH 8.0, 150 mM NaCl), blocked and permeabilized overnight at 4°C in Odyssey Blocking Buffer (LI-COR Biosciences, Lincoln, NE, USA) containing 0.1% Tween-20 and 1 mM sodium orthovanadate. Slices were incubated at 4°C for 18 h with primary antibodies: CB_1 cannabinoid receptor (CB_1R, Santa Cruz Biotechnology, Santa Cruz, CA, USA; 1 : 750), CRIP1a (AbK148; 1 : 300; AbD20; 1 : 300), D_2 dopamine receptor (D_2DR, Santa Cruz; 1 : 500), D_1 dopamine receptor (D_1DR, Santa Cruz; 1 : 300), delta opioid receptor 1 (DOR1, Santa Cruz; 1 : 500), mu opioid receptor 1(MOR1, Santa Cruz; 1 : 500), total ERK1/2 (ERK2, Santa Cruz; 1 : 1000), phosphoERK1/2 (p-ERK, Santa Cruz; 1 : 500), total CREB (CREB, Cell Signaling; 1 : 1000), phosphoCREB (p-CREB, Cell Signaling; 1:500). Slices were washed in TBS containing 0.1% Tween 20 (TBS-T), and incubated for 2 h with a secondary goat anti-rabbit (1:1500) or goat anti-mouse antibody (1 : 1500) conjugated to

infrared dyes, washed in TBS-T and allowed to dry overnight. The fluorescent immunocomplexes were detected using the LI-COR Odyssey imaging system and software program (LI-COR Biosciences, Lincoln, NE, USA), and integrated densities from gray-scale images were determined for demarcated regions of interest (dorsal striatum, globus pallidus, entopeduncular nucleus) using Image J software (National Institutes of Health, Bethesda, MD, USA, http://rsb.info.nih.gov/ij/) (see Figure S1D, E, F). Changes in protein levels were determined by comparing the integrated densities between the AAV-treated and the untreated contralateral hemisphere. For phospho-CREB and phospho-ERK levels, normalization was established to total CREB or ERK, respectively.

[^{35}S]GTPγS binding in brain slices

Agonist-induced G protein activation by CB_1R, D_2R, MOR1, and DOR1 was quantitated by [^{35}S]GTPγS, binding assays. Receptor/G protein coupling was assayed in rat brain sections using [^{35}S]GTPγS autoradiography (Sim *et al.* 1995). Rat brain sections (20 μm) were pre-incubated for 10 min in TME buffer (50 mM Tris-HCl, 3 mM $MgCl_2$, 0.2 mM EGTA, 100 mM NaCl, pH 7.4), then 15 min with 1 mM GDP and 1 μM DPCPX at 25°. Sections were incubated in assay buffer with 1 mM GDP and 1 μM DPCPX, 0.04 nM [^{35}S] GTPγS, with or without various agonists for 2 h at 25°. Agonists included 1 μM WIN 55212-2 (CB_1R), 3 μM NPA (D_2R), 3 μM DAMGO (mu opioid), and 3 μM DPDPE (delta opioid). The sections were then washed, exposed to X-ray film, and analyzed as described previously (Sim *et al.* 1995). Agonist-stimulated activity was calculated by subtracting the optical density in basal sections (GDP only) from that of agonist-stimulated sections and results are expressed as percent stimulation over basal activity.

Statistical analyses

Data from treated (ipsilateral) sides of the brain were compared to untreated control tissue isolated from the same region on the contralateral side of the brain, such that each animal served as its own control. Statistical differences were determined by paired comparisons between treated and untreated tissue using Student's paired two-sided *t*-test analyses on Prism 4 or InStat software (GraphPad Software Inc., San Diego, CA, USA).

Results

AAV-shRNA-mediated CB_1R and D_2R knockdown *in vivo*

CB_1Rs are expressed in the GABAergic MSNs of the striatum that project both directly and indirectly to their output nuclei (Herkenham *et al.* 1991; Mailleux and Vanderhaeghen 1992; Martin *et al.* 2008). The MSNs of the direct pathway express D_1 receptors (striatonigral pathway), whereas the MSNs of the indirect pathway preferentially express D_2 receptors (striatopallidal) (Hermann *et al.* 2002; Pickel *et al.* 2006; Tepper *et al.* 2007). Our goal was to directly and selectively manipulate the expression of either CB_1Rs or D_2Rs in the dorsal striatum to determine the extent to which these receptors regulate signal transduction and gene expression in intact basal ganglia tissue.

We characterized the kinetics of CB_1R and D_2R knock-down by shRNA designed specifically against either CB_1R or D_2R. The AAV2/10 virus transduces the cell bodies at the injection site, and is not further delivered by trans-synaptic mechanisms (Xiao *et al.* 1998). A single unilateral injection of AAV-shCB_1R in the rat dorsal striatum produced a reduction in CB_1R mRNA levels to 58 ± 4% compared to control at day 21, and remained significantly reduced to day 56. Analysis of AAV-shCB_1R-treated striata revealed a time-dependent reduction in D_2R mRNA that accompanied the reductions observed for CB_1R mRNA (Fig. 1a). Injection of AAV-shD_2R into dorsal striatum resulted in noticeable reductions in D_2R mRNA levels starting at day 3 (15 ± 3%) and continuing until day 56 (23

± 6%). The maximum decline in D_2R transcript levels that AAV-shD_2R was capable of producing occurred between days 10 and 28 (52 ± 6%) (Fig. 1b). Interestingly, CB_1R transcript levels were significantly reduced as a result of knockdown of D_2Rs in rat striatum (Fig. 1b). It appears that the transcriptional regulation or mRNA stability of these receptors is tightly coupled, as AAV-mediated knockdown of one receptor coincides with mRNA reductions in the other receptor.

Using an immunohistochemistry procedure that could quantify receptor protein in identified regions of interest in brain slices, we established the extent of receptor protein loss following AAV-mediated knockdown of CB_1Rs or D_2Rs. Because maximum knockdown of CB_1R and D_2R mRNA occurred between days 15 and 30, we examined immunoreactive receptor densities in slices from brains at 17 days post-injection of AAV-shCB_1R or AAV-shD_2R. Comparison of regions of interest (see Figure S1) between ipsilateral (injected) and contralateral (non-injected) hemispheres from AAV-shCB_1R- injected animals showed a significant decrease in CB_1R immunoreactive protein in the dorsal striatum (21 ± 5%), as well as in the outflow projections to the globus pallidus (13 ± 2%) and entopeduncular nucleus (26 ± 3%) (Fig. 1c). This is consistent with a scenario of CB_1R synthesis in cell bodies of striatal MSNs, and subsequent translocation to the pre-synaptic termini in the 'indirect' pathway of the basal ganglia [see review (Mackie 2005)]. As seen with transcript levels, knockdown of the CB_1R was associated with a statistically significant reduction in D_2R protein in the dorsal striatum (15 ± 6%) and entopeduncular nucleus (17 ± 3%), with a decrease within the globus pallidus (8 ± 1%) (Fig. 1c).

Brain slices from rat dorsal striata injected with AAV-shD_2R exhibited a significant knockdown of immunoreactive D_2R in the dorsal striatum (35 ± 6%), globus pallidus (16 ± 1%), and entopeduncular nucleus (16 ± 2%) (Fig. 1d). Significant reductions of immunoreactive CB_1R were observed in the dorsal striatum (14 ± 6%) and entopeduncular nucleus (18 ± 4%), as well as a reduction in the globus pallidus (8 ± 1%) (Fig. 1d). Although a parallel relationship was observed between CB_1R and D_2R knockdown, specific knockdown of either receptor failed to alter D_1R transcript levels (data not shown) or total protein levels (Fig. 1c and d). This evidence supports the notion that whereas CB_1Rs exert a regulatory influence on D_2Rs in the "indirect" pathway, there is very limited or no regulation of the D_1 receptor system in neurons comprising the 'direct' pathway in the basal ganglia.

AAV-CRIP1a-mediated CRIP1a over-expression *in vivo*

Analysis of dorsal striatal tissue from AAV-shCB_1R or AAV-shD_2R-treated animals revealed that knockdown of CB_1Rs and D_2Rs induced a 3- and 4-fold increase in the mRNA levels of CRIP1a, respectively (Fig. 1a and b). These increases in CRIP1a mRNA were accompanied by an approximately 25% increase in levels of CRIP1a immunoreactive protein in the dorsal striatum as well as significant, but less robust, increases in the outflow nuclei (Fig. 1c and d). Interestingly, the time-course for the increase in striatal CRIP1a mRNA and protein mirrored the decreases in striatal CB_1R and D_2R mRNA and protein. Our data showing increased levels of protein in the outflow nuclei of the dorsal striatum suggest that CRIP1a gains access to the axonal compartment and can establish a synthesis/degradation equilibrium at that locus as well as at the cell soma.

As striata from both AAV-shCB_1R- and AAV-shD_2R-injected animals displayed a marked increase in CRIP1a mRNA and protein levels, we took the complimentary approach of over-expressing CRIP1a *in vivo* to investigate its role in the regulation of CB_1R- and D_2R-mediated functions in rat striatum. AAV-CRIP1a was unilaterally injected into the rat dorsal striatum and differences in gene expression between ipsilateral and contralateral hemispheres were assessed 3, 5, 10, and 17 days post-injection. CRIP1a mRNA levels were

significantly increased at all measured time-points. Striata from AAV-CRIP1a-injected rats displayed 5- to 6-fold increases in levels of CRIP1a transcript as early as 3 days and at least as long as 17 days post-injection (the last time-point examined) (Fig. 2a). During this time-course, no measurable deviations in the expression of D_2R mRNA were detected when compared to the contralateral hemisphere (Fig. 2a). However, CB_1R mRNA increased transiently at the day 3 time-point following the AAV-CRIP1a injection, before returning to pre-injection expression levels at day 5 (Fig. 2a).

Viral delivery of shRNA transgenes has been shown to induce immunomodulatory responses at the injection site with some, but not all, shRNA sequences (McBride *et al.* 2008). Evidence suggests that CB_1R expressed by both glia and microglia participate in immune responses (Klein *et al.* 2003; Cabral and Marciano-Cabral 2005; Sheng *et al.* 2005). Thus, we hypothesized that the transient CB_1R up-regulation seen within the earliest days following the AAV-CRIP1a injection might be because of the infiltration of immune cells and/or gliosis in response to the viral injection. To investigate this, RNA from the injection sites of AAV-shCB_1R, AAV-shD_2R, and AAV-CRIP1a animals were subjected to qPCR, and analyzed for glial fibrillary acidic protein (GFAP), an astrocytic marker (Smith and Eng 1987) and IBA1, a protein specifically expressed and up-regulated during macrophage/microglia activation (Ito *et al.* 2001). Analysis of striatal gene expression from AAV-injected animals showed that the mRNA levels of GFAP and IBA1 were significantly increased at only the day 3 time-point and returned to baseline by day 5 (data not shown). Of particular note, control rats injected intra-striatally with vehicle (Dulbecco's Modified Eagle's Medium) or AAV-shScramble also displayed increased GFAP and IBA1 expression at the day 3 time-point only, compared with the control brain hemispheres, in which the microglial marker IBA1 was expressed at levels that were 1% of eno2 (data not shown). These findings suggest that the short-lived immune response results from the injection process itself, indicative of inflammatory cell infiltration immediately following the injection. During the time-course of the study, no statistical differences in eno2 were detected between the ipsilateral and contralateral hemispheres. This finding indicates that no decreases in neuronal mass, characteristic of neurodegeneration, were investigated in response to the AAV injection.

For detection of CRIP1a protein, we generated CRIP1a AbD20 (see Figure S2). Rats were killed at 17 days post-injection with AAV-CRIP1a, by which time AAV-mediated transgene expression had peaked and reached equilibrium. AAV-CRIP1a successfully over-expressed CRIP1a protein levels over a 17-day time period, not only in the striatum (42 ±8%) but also in the globus pallidus (43 ±5%) and entopeduncular nucleus (42 ±6%) (Fig. 2b). However, no detectable, sustained differences in CB_1R, D_2R or D_1R mRNA or protein levels were observed as a result of over-expression of CRIP1a in the dorsal striatum (Fig. 2a and b). The lack of changes in CB_1R or D_2R levels indicates a non- reciprocal relationship between the expression patterns of these proteins *in vivo*.

CB_1R and D_2R knockdown influence G protein activation and signal transduction

To investigate the effects of AAV-shCB_1R and AAV-shD_2R knockdown and CRIP1a over-expression on receptor-stimulated G protein activation, [^{35}S]GTPγS binding assays were performed on coronal brain slices from animals killed 17 days post-injection. Knockdown of either the D_2R or CB_1R in the striatum was associated with a 19 ± 7% or 19 ± 4% reduction, respectively, of striatal NPA [3 μM]-stimulated G protein activation (Fig. 3a). No appreciable changes in D_2R-stimulated G protein activation were observed following striatal over-expression of CRIP1a. Fig. 3b shows the effects of CB_1R and D_2R knockdown and CRIP1a over-expression on [^{35}S]GTPγS binding stimulated by the CB_1R agonist WIN55212 in the globus pallidus. Striatal knockdown of CB_1Rs did not result in measurable differences in CB_1R-stimulated [^{35}S]GTPγS binding in the globus pallidus, the site of pre-

synaptic CB_1R (Fig 3b). The lack of significant reduction in WIN55212-stimulated [^{35}S]GTPγS binding may be attributed to the expression of CB_1R in post-synaptic globus pallidus neurons, which would not have been altered by the knockdown of the pre-synaptic CB_1Rs. D_2R knockdown significantly reduced CB_1R-stimulated G protein activation (17 ± 3%) in the globus pallidus, an effect that could represent the response of either pre-synaptic because of direct effects of the CB_1R or post-synaptic neurons because of the effects of released neurotransmitters (Fig. 3b). CRIP1a over-expression produced a 16± 8% decrease in CB_1R-stimulated [^{35}S]GTPγS binding in the globus pallidus.

Effects of AAV-shCB_1R and AAV-shD_2R knockdown and CRIP1a over-expression on levels of phosphoCREB and phosphoERK were quantitated in rats killed at 17 days post-treatment. Comparison of immunofluorescence between hemispheres on coronal brain slices showed that the total protein levels of ERK1/2 and CREB were not affected following any of the viral injections performed (data not shown); therefore, phosphoERK and phosphoCREB immunostaining could be normalized to the total ERK and CREB protein. Striatal CB_1R knockdown was associated with a significant decrement in phosphoERK levels in the striatum (18 ± 3%) as well as the outflow projections to the globus pallidus (17 ± 2%) and entopeduncular nucleus (21 ± 2%), reflecting changes in either pre-synaptic or post-synaptic signal transduction or both (Fig. 3c). CRIP1a over-expression in the dorsal striatum was also associated with a marked reduction in phosphoERK levels in the striatum (16 ± 3%), globus pallidus (17 ± 4%) and entopeduncular nucleus (15 ± 1%) (Fig. 3c). The levels of phosphoCREB were not altered by striatal CB_1R knockdown or CRIP1a over-expression (Fig. 3d), suggesting that, in contrast to ERK, CREB regulation may not be a mechanism for CB_1R regulation of gene expression within neurons in either the striatum or the post-synaptic neurons in the outflow nuclei.

Striatal D_2R knockdown had a region-specific effect on the phosphoERK levels, such that levels of phosphoERK were reduced in the striatum (18 ± 2%), but significantly increased in the globus pallidus (11 ± 2%) and entopeduncular nucleus (11 ± 3%) (Fig. 3c). The levels of phospho-CREB were not altered by D_2R-knockdown, except in the globus pallidus, where a significant increase in phospho-CREB (9 ± 1%) was observed (Fig. 3d). As phosphoCREB is likely to be found in nuclei of the post-synaptic neurons, one could postulate that increases in both phospho-ERK and phosphoCREB are occurring in post-synaptic neurons associated with D_2R reduction in the striatal MSNs.

Striatal CB_1R and D_2R evoke regulation of opioid peptide systems

As CB_1R and D_2R are co-expressed and co-localized in the enkephalin-containing GABAergic MSNs of the striatum (Pickel *et al.* 2006), we sought to identify downstream influences exerted by CB_1R and D_2R knockdown on opioid physiology. Within days following striatal knockdown of either CB_1R or D_2R, the mRNA expression of opioid peptide precursors PENK and PDYN in the dorsal striatum was significantly decreased (Fig. 4a and b). Gene expression of the delta (DOR1) but not mu (MOR1) opioid receptor was increased in the same striatal tissue samples. Time-course analysis indicated that mRNA levels of DOR1 were up-regulated within 7 days after the maximum reduction of PENK associated with D_2R knockdown (Fig. 4b). CRIP1a over-expression also evoked significant reductions in PENK and PDYN transcript levels, and within days, mRNA levels of DOR1 were significantly up-regulated (Fig. 4c). There were no significant alterations in the gene expression of MOR1 at any time-point. This time-course suggested that an alteration in the synthesis or degradation of DOR1 followed a change in availability of the endogenous agonist enkephalin. These observations might suggest a direct effect on gene expression or mRNA stability within neurons, such that modifications in CB_1R, D_2R, or CRIP1a levels contribute to the suppression of opioid peptides concurrently with increased expression of DOR1. Alternatively, a decrease in enkephalin leading to reduced local DOR1 stimulation

might trigger DOR1 up-regulation. Finally, a multi-cellular regulatory mechanism may come into play in the dorsal striatum.

CB_1R, D_2R, and CRIP1a influence DOR1 protein levels and signal transduction

We investigated the responses to opioid transcriptional alterations with studies on MOR1 and DOR1 receptor expression and function. Fig. 5a shows that there were no changes in the immunoreactive protein levels of MOR1 at 17 day post-injection of any of the AAV transcripts. Striatal CB_1R knockdown animals displayed significant increases in immunoreactive DOR1 protein in the dorsal striatum (25 ± 7%), globus pallidus (25 ± 6%), and entopeduncular nucleus (21 ± 7%). Striatal D_2R knockdown resulted in significant increases in DOR1 protein in the striatum (27 ± 6%) and globus pallidus (15 ± 4%), and a notable increase in the entopeduncular nucleus (10 ± 4%) that trended toward significant at $p < 0.10$. CRIP1a over-expression resulted in significantly increased DOR1 protein in the dorsal striatum (18 ± 5%), globus pallidus (11 ± 2%), and entopeduncular nucleus (23 ±3%) (Fig. 5b).

To determine if these receptors were functionally coupled to Gi/o proteins, we evaluated agonist-stimulated G protein activation. D_2R knockdown and CRIP1a over-expression produced significant increases in DPDPE-stimulated [^{35}S] GTPγS binding in dorsal striatum (43 ±14%; 29 ±5%, respectively) (Fig. 5c). Although knockdown of CB_1R resulted in significantly increased striatal DOR1 protein (27 ±8%), no changes were observed in DPDPE-stimulated [^{35}S]GTPγS binding. Neither CB_1R or D_2R knockdown, nor CRIP1a over-expression exerted any significant effect on DAMGO-stimulated [^{35}S]GTPγS binding in the dorsal striatum (Fig. 5c).

Discussion

Physiological and biochemical evidence for the interaction between cannabinoid and dopamine receptor systems has continued to accumulate over the last two decades [reviewed in (Fernandez-Ruiz *et al.* 2010)]. Despite their close pharmacological interactions, few studies have directly investigated the biological underpinnings involved in the synthesis and expression of CB_1R and D_2R during manipulation of the other receptor. In this study, we utilized RNA interference to inhibit the synthesis of CB_1R or D_2R in rat dorsal striatum to investigate the interactions between cannabinoid, dopamine, and opioid receptor systems.

These studies demonstrate that CB_1R and D_2R are tightly coupled at the transcript, protein and signaling level in rat dorsal striatum. The knockdown of either CB_1R or D_2R resulted in the concomitant suppression of the expression of the other receptor in the cell bodies of the dorsal striatum and in the projections to the globus pallidus and entopeduncular nucleus. It is reasonable to postulate that the decrease in receptors in the outflow nuclei was because of the use-dependent, agonist-driven processes of internalization and degradation of pre-synaptic receptors, coupled with the reduced ability to replenish these receptors as a result of the RNA interference at the soma. Our data suggest that a new equilibrium is established within 15–30 days, after which, the RNA interference becomes less effective and the equilibrium tends to become re-established toward control at the end of the 56-day post-injection period.

Consistent with our findings, studies of subchronic pharmacological blockade of the D_2R in rats with the antagonist haloperidol resulted in an increase in striatal D_2R binding and G protein activation as expected with decreased use, but also an increase in striatal CB_1R binding and G protein activation in the outflow nuclei (Andersson *et al.* 2005). Levels of D_2R in the dorsal striatum in response to subchronic pharmacological blockade of the CB_1R with rimonabant were increased in rats (Crunelle *et al.* 2011). Combined electrophysical and

biochemical studies demonstrate that activation of the striatal dopaminergic system up-regulates anandamide and CB_1 receptor levels in the striatum, and CB_1R has been postulated to be a downstream effector of D_2 receptors in the inhibition of GABAergic neurotransmission (Centonze *et al.* 2004). Our results suggest a coupling of the regulation and expression between CB_1R and D_2R, and as such may provide insight into reward and learning based mechanisms where induction of corticostriatal long-term depression (Gerdeman *et al.* 2002) or striatal synaptic plasticity is of underlying importance (i.e., drug addiction and motor movement disorders).

In contrast to our current findings, genetic deletion using knockout mice indicated that the expression of CB_1R and D_2R was inversely related. Life-long, total loss of CB_1R resulted in up-regulated expression of D_2R in the striatum (Houchi *et al.* 2005), probably as the result of developmental compensatory alterations in the $GABA_A$ and NMDA receptors in the basal ganglia circuitry of CB_1R knockout mice (Warnault *et al.* 2007). Life-long, total loss of D_2R resulted in up-regulated expression of CB_1R in the striatum (Thanos *et al.* 2011). The general conclusion from these studies is that loss of cannabinergic or dopaminergic signaling is compensated through the up-regulation of the other receptor system to maintain functional homeostasis as the basal ganglia circuitry develops. Our examination of homeostatic mechanisms in response to partial CB_1R or D_2R knockdown in normal adult animals after the basal ganglia circuitry has already been established, may be more reminiscent of adult neurodegenerative diseases such as Huntington's disease, in which the MSNs suffer a loss of CB_1R and D_2R concurrently early in their degeneration process (Glass *et al.* 2000; Blazquez *et al.* 2011). Also in contrast to knockout mice, the clearly delineated AAV-shRNA injection locus allows receptor knockdown to be limited to cell soma within the dorsal striatum, and thus, CB_1R on glutamatergic terminals and D_2R on nigrostriatal terminals are not targeted.

The partial deficit observed in striatal D_2R, evoked by either D_2R or CB_1R knockdown, was reflected in comparable decrements in D_2R-G protein activation and reductions in phosphoERK levels in the dorsal striatum. In contrast, the shRNA-mediated deficit in D_2R in the globus pallidus was associated with increased phosphoERK as well as phospho-CREB, indicative of signal transduction in the post-synaptic neurons, perhaps because of an amelioration of D_2R-mediated suppression of neurotransmission. As knockdown of CB_1R or D_2R failed to alter D_1R transcript, protein or receptor activity, the dynamic changes in receptor expression, activity, and downstream signaling to the ERK pathway appear to be selective for the D_2R-positive striatopallidal pathway.

Our findings are unique in reporting an interaction between CB_1R and D_2R at the transcript level in the striatum. Gene expression of neuronal CB_1R can be regulated by ERK (Lim *et al.* 2003), a potential signaling mechanism by which D_2R could influence the expression at the transcription level. Similarly, ERK was able to stimulate the D_2R promoter (Takeuchi *et al.* 2002), providing a common mechanism by which both receptors might be regulated concurrently.

We also identified an augmentation in expression of CRIP1a, a CB_1R-associated protein that interacts with the distal carboxy terminus of CB_1R, but not CB_2R (Niehaus *et al.* 2007), whose role in cellular physiology has remained elusive. Although a direct functional link between CRIP1a and CB_1R has yet to be established, the mRNA levels of both CRIP1a and CB_1R were reduced in epileptic hippocampal tissue compared with control, likely associated with decreased CB_1Rs in glutamatergic terminals (Ludanyi *et al.* 2008). Immunofluorescence staining indicated that CRIP1a was in close proximity to CB_1R in the pre-synaptic terminals of retina cone photoreceptors (Hu *et al.* 2010).

Our data on CRIP1a expression revealed the presence of CRIP1a transcript and protein in the striatum, globus pallidus, and entopeduncular nucleus, comprising the striatopallidal pathway. Knockdown of either CB_1Rs or D_2Rs resulted in up-regulation of CRIP1a transcript and protein, suggesting a novel role for the CRIP1a protein in dopamine receptor systems. We hypothesized that the observed changes in CRIP1a could be related mechanistically to the cellular signaling patterns of CB_1Rs and D_2Rs, and developed a CRIP1a over-expressing virus to evaluate this hypothesis. CRIP1a over-expression reduced phosphoERK in the striatum and its outflow projections, recapitulating the effects of CB_1R knockdown. Niehaus and colleagues (Niehaus *et al.* 2007) suggested that the physiological role of CRIP1a was to reduce CB_1R-mediated tonic inhibition of Ca^{2+} channels, but data supporting effects on other CB_1R-mediated responses is just beginning to be appreciated. One possible mechanism by which CRIP1a could reduce ERK phosphorylation is indirectly through CRIP1a regulation of CB_1R signaling, inasmuch as our data indicate that there were no effects of CRIP1a over-expression on CB_1R mRNA or protein levels. This finding is consistent with data from cotransfected cell lines, which also showed no effect on CB_1R expression when CRIP1a was over-expressed (Niehaus *et al.* 2007).

A prominent finding was the down-regulation of mRNA for the opioid peptides PDYN and PENK that accompanied knockdown of CB_1Rs or D_2Rs. The down-regulation in opioid peptide mRNAs was followed in time by increased DOR1 mRNA expression and augmented protein expression along the striatopallidal pathway. Interestingly, these same sequelae were mimicked by over-expression of CRIP1a. Data from our lab in N18TG2 neuronal cells stably over-expressing CRIP1a shows that PENK mRNA is significantly reduced and concomitantly DOR1 mRNA is up-regulated when compared with WT cells (Blume *et al.* 2010). A possible mechanism for the observed changes in opioid physiology is that CB_1Rs, D_2Rs (and suppressed CRIP1a levels) contribute to the expression of opioid peptides in MSNs. Intra-striatal administration of selective inhibitors of ERK phosphorylation blocked opioid peptide gene expression in rats (Shi and McGinty 2006). Thus, one possible mechanism for the observed reductions in PENK and PDYN gene expression may be related to the reduction in striatal ERK phosphorylation resulting from CB_1R or D_2R knockdown, and CRIP1a over-expression. Reduced enkephalin-stimulated DOR1 may lead to DOR1 up-regulation, as increased DOR1 binding has been observed in quantitative autoradiography studies in enkephalin knockout mice (Brady *et al.* 1999). Alternatively, the observed up-regulation in DOR1 expression may be an adaptive response that mediates recovery of the disinhibition of the striatopallidal pathway produced by the loss of CB_1Rs and/or D_2Rs receptors in the dorsal striatum.

The ability to achieve specific time-dependent knockdown of CB_1Rs and D_2Rs in a discrete population of basal ganglia neurons is a significant advantage over knockout mice in the investigation of pathologies where reductions, but not total loss of CB_1R or D_2R is observed. This study may have therapeutic relevance in diseases of the basal ganglia in which CB_1Rs and D_2Rs are key players in the underlying pathophysiology, such as Parkinson's and Huntington's diseases as well as drug addiction. The present data add to a growing body of evidence for a cellular and molecular interaction between CB_1Rs and D_2Rs at the behavioral, systems, and cellular-molecular levels.

Supplementary Material

Refer to Web version on PubMed Central for supplementary material.

Acknowledgments

This study was supported by US Public Health Services grants: R01-DA03690; R01 DA014030 R21-DA025321; K01-DA024763, P50-DA006634, F32-DA026295, T32-DA00724, and F31-DA032215.

Abbreviations used

AAV	adeno-associated virus
CREB	cAMP-response element binding protein
CRIP1a	cannabinoid receptor interacting protein 1a
DAMGO	[D-Ala2, NMe-Phe4, Gly-ol5]-enkephalin
DPDPE	[D-Pen2, D-Pen5]-enkephalin
EGFP	enhanced green fluorescent protein
GFAP	glial fibrillary acidic protein
MSN	medium spiny neurons
NPA	*N*-propylnorapomorphine
PDYN	pro-dynorphin
PENK	pro-enkephalin
TBS	Tris-buffered saline

References

Andersson M, Terasmaa A, Fuxe K, Stromberg I. Subchronic haloperidol increases CB(1) receptor binding and G protein coupling in discrete regions of the basal ganglia. J Neurosci Res. 2005; 82:264–272. [PubMed: 16175569]

Blazquez C, Chiarlone A, Sagredo O, et al. Loss of striatal type 1 cannabinoid receptors is a key pathogenic factor in Huntington's disease. Brain. 2011; 134:119–136. [PubMed: 20929960]

Blume LC, Bass CE, Dalton GD, Selley DE, Howlett AC. Cannabinoid receptor interacting protein (CRIP) 1a: signal transduction and epigenetic phenomena. ICRS Symp Cannabinoids. 2010; 20:P3–P30.

Brady LS, Herkenham M, Rothman RB, Partilla JS, Konig M, Zimmer AM, Zimmer A. Region-specific up-regulation of opioid receptor binding in enkephalin knockout mice. Brain Res Mol Brain Res. 1999; 68:193–197. [PubMed: 10320798]

Cabral GA, Marciano-Cabral F. Cannabinoid receptors in microglia of the central nervous system: immune functional relevance. J Leukoc Biol. 2005; 78:1192–1197. [PubMed: 16204639]

Centonze D, Battista N, Rossi S, Mercuri NB, Finazzi-Agro A, Bernardi G, Calabresi P, Maccarrone M. A critical interaction between dopamine D2 receptors and endocannabinoids mediates the effects of cocaine on striatal GABAergic transmission. Neuropsychopharmacology. 2004; 29:1488–1497. [PubMed: 15100701]

Crespo I, de Gomez H, Rodriguez de FFR, Navarro M. Pretreatment with subeffective doses of Rimonabant attenuates orexigenic actions of orexin A-hypocretin 1. Neuropharmacology. 2008; 54:219–225. [PubMed: 17889909]

Crunelle CL, van de Giessen E, Schulz S, Vanderschuren LJ, de BK, van den Brink W, Booij J. Cannabinoid-1 receptor antagonist rimonabant (SR141716) increases striatal dopamine D2 receptor availability. Addict Biol. 201110.1111/j.1369-1600.2011.00369.x

De BP, Heguy A, Hackett NR, Ferris B, Leopold PL, Lee J, Pierre L, Gao G, Wilson JM, Crystal RG. High levels of persistent expression of alpha1-antitrypsin mediated by the nonhuman primate serotype rh. 10 adeno-associated virus despite preexisting immunity to common human adeno-associated viruses. Mol Ther. 2006; 13:67–76. [PubMed: 16260185]

Elphick MR, Wallis KT, Liu Y, Lewis DL, Egertova. Localization of the CB1 cannabinoid receptor interacting protein (CRIP1a) in the brain. ICRS Symp Cannabinoids. 2004; 14:19.

Fernandez-Ruiz J. The endocannabinoid system as a target for the treatment of motor dysfunction. Br J Pharmacol. 2009; 156:1029–1040. [PubMed: 19220290]

Fernandez-Ruiz J, Hernandez M, Ramos JA. Cannabinoid-dopamine interaction in the pathophysiology and treatment of CNS disorders. CNS Neurosci Ther. 2010; 16:e72–e91. [PubMed: 20406253]

Gao GP, Alvira MR, Wang L, Calcedo R, Johnston J, Wilson JM. Novel adeno-associated viruses from rhesus monkeys as vectors for human gene therapy. Proc Natl Acad Sci USA. 2002; 99:11854–11859. [PubMed: 12192090]

Gerald TM, Ward GR, Howlett AC, Franklin SO. CB1 knockout mice display significant changes in striatal opioid peptide and D4 dopamine receptor gene expression. Brain Res. 2006; 1093:20–24. [PubMed: 16684513]

Gerdeman GL, Ronesi J, Lovinger DM. Postsynaptic endocannabinoid release is critical to long-term depression in the striatum. Nat Neurosci. 2002; 5:446–451. [PubMed: 11976704]

Gerfen CR, Engber TM, Mahan LC, Susel Z, Chase TN, Monsma FJ Jr, Sibley DR. D1 and D2 dopamine receptor-regulated gene expression of striatonigral and striatopallidal neurons. Science. 1990; 250:1429–1432. [PubMed: 2147780]

Glass M, Felder CC. Concurrent stimulation of cannabinoid CB1 and dopamine D2 receptors augments cAMP accumulation in striatal neurons: evidence for a Gs linkage to the CB1 receptor. J Neurosci. 1997; 17:5327–5333. [PubMed: 9204917]

Glass M, Dragunow M, Faull RL. The pattern of neurodegeneration in Huntington's disease: a comparative study of cannabinoid, dopamine, adenosine and GABA(A) receptor alterations in the human basal ganglia in Huntington's disease. Neuroscience. 2000; 97:505–519. [PubMed: 10828533]

Herkenham M, Lynn AB, De Costa BR, Richfield EK. Neuronal localization of cannabinoid receptors in the basal ganglia of the rat. Brain Res. 1991; 547:267–274. [PubMed: 1909204]

Hermann H, Marsicano G, Lutz B. Coexpression of the cannabinoid receptor type 1 with dopamine and serotonin receptors in distinct neuronal subpopulations of the adult mouse forebrain. Neuroscience. 2002; 109:451–460. [PubMed: 11823058]

Houchi H, Babovic D, Pierrefiche O, Ledent C, Daoust M, Naassila M. CB1 receptor knockout mice display reduced ethanol-induced conditioned place preference and increased striatal dopamine D2 receptors. Neuropsychopharmacology. 2005; 30:339–349. [PubMed: 15383833]

Hu SS, Arnold A, Hutchens JM, Radicke J, Cravatt BF, Wager-Miller J, Mackie K, Straiker A. Architecture of cannabinoid signaling in mouse retina. J Comp Neurol. 2010; 518:3848–3866. [PubMed: 20653038]

Ito D, Tanaka K, Suzuki S, Dembo T, Fukuuchi Y. Enhanced expression of Iba1, ionized calcium-binding adapter molecule 1, after transient focal cerebral ischemia in rat brain. Stroke. 2001; 32:1208–1215. [PubMed: 11340235]

Jarrahian A, Watts VJ, Barker EL. D2 dopamine receptors modulate Galpha-subunit coupling of the CB1 cannabinoid receptor. J Pharmacol Exp Ther. 2004; 308:880–886. [PubMed: 14634050]

Kearn CS. Immunofluorescent mapping of cannabinoid CB1 and dopamine D2 receptors in the mouse brain. LI-COR Biosci, Application Notes. 2004

Kearn CS, Blake-Palmer K, Daniel E, Mackie K, Glass M. Concurrent stimulation of cannabinoid CB1 and dopamine D2 receptors enhances heterodimer formation: a mechanism for receptor cross-talk? Mol Pharmacol. 2005; 67:1697–1704. [PubMed: 15710746]

Kilkenny C, Browne WJ, Cuthill IC, Emerson M, Altman DG. Improving bioscience research reporting: the ARRIVE guidelines for reporting animal research. J Pharmacol Pharmacother. 2010; 1:94–99. [PubMed: 21350617]

Klein TW, Newton C, Larsen K, Lu L, Perkins I, Nong L, Friedman H. The cannabinoid system and immune modulation. J Leukoc Biol. 2003; 74:486–496. [PubMed: 12960289]

Lim G, Sung B, Ji RR, Mao J. Upregulation of spinal cannabinoid-1-receptors following nerve injury enhances the effects of Win 55,212–2 on neuropathic pain behaviors in rats. Pain. 2003; 105:275–283. [PubMed: 14499445]

Lovinger DM. Neurotransmitter roles in synaptic modulation, plasticity and learning in the dorsal striatum. Neuropharmacology. 2010; 58:951–961. [PubMed: 20096294]

Ludanyi A, Eross L, Czirjak S, Vajda J, Halasz P, Watanabe M, Palkovits M, Magloczky Z, Freund TF, Katona I. Downregulation of the CB1 cannabinoid receptor and related molecular elements of the endocannabinoid system in epileptic human hippocampus. J Neurosci. 2008; 28:2976–2990. [PubMed: 18354002]

Mackie K. Distribution of cannabinoid receptors in the central and peripheral nervous system. Handb Exp Pharmacol. Vol. 2005; 168:299–325.

Mailleux P, Vanderhaeghen JJ. Localization of cannabinoid receptor in the human developing and adult basal ganglia. Higher levels in the striatonigral neurons. Neurosci Lett. 1992; 148:173–176. [PubMed: 1300492]

Marcellino D, Carriba P, Filip M, et al. Antagonistic cannabinoid CB1/dopamine D2 receptor interactions in striatal CB1/D2 heteromers.a combined neurochemical and behavioral analysis. Neuropharmacology. 2008; 54:815–823. [PubMed: 18262573]

Martin AB, Fernandez-Espejo E, Ferrer B, Gorriti MA, Bilbao A, Navarro M, de Rodriguez FF, Moratalla R. Expression and function of CB1 receptor in the rat striatum: localization and effects on D1 and D2 dopamine receptor-mediated motor behaviors. Neuropsychopharmacology. 2008; 33:1667–1679. [PubMed: 17957223]

Matyas F, Yanovsky Y, Mackie K, Kelsch W, Misgeld U, Freund TF. Subcellular localization of type 1 cannabinoid receptors in the rat basal ganglia. Neuroscience. 2006; 137:337–361. [PubMed: 16289348]

McBride JL, Boudreau RL, Harper SQ, et al. Artificial miRNAs mitigate shRNA-mediated toxicity in the brain: implications for the therapeutic development of RNAi. Proc Natl Acad Sci USA. 2008; 105:5868–5873. [PubMed: 18398004]

Meschler JP, Howlett AC. Signal transduction interactions between CB1 cannabinoid and dopamine receptors in the rat and monkey striatum. Neuropharmacology. 2001; 40:918–926. [PubMed: 11378162]

Niehaus JL, Liu Y, Wallis KT, et al. CB1 cannabinoid receptor activity is modulated by the cannabinoid receptor interacting protein CRIP 1a. Mol Pharmacol. 2007; 72:1557–1566. [PubMed: 17895407]

Paxinos, G.; Watson, C. The Rat Brain in Stereotaxic Coordinates. Academic Press; New York: 1997.

Pickel VM, Chan J, Kearn CS, Mackie K. Targeting dopamine D2 and cannabinoid-1 (CB1) receptors in rat nucleus accumbens. J Comp Neurol. 2006; 495:299–313. [PubMed: 16440297]

Przybyla JA, Watts VJ. Ligand-induced regulation and localization of cannabinoid CB1 and dopamine D2L receptor heterodimers. J Pharmacol Exp Ther. 2010; 332:710–719. [PubMed: 20016021]

Sadri-Vakili G, Kumaresan V, Schmidt HD, et al. Cocaine-induced chromatin remodeling increases brain-derived neurotrophic factor transcription in the rat medial prefrontal cortex, which alters the reinforcing efficacy of cocaine. J Neurosci. 2010; 30:11735–11744. [PubMed: 20810894]

Sanudo-Pena MC, Tsou K, Walker JM. Motor actions of cannabinoids in the basal ganglia output nuclei. Life Sci. 1999; 65:703–713. [PubMed: 10462071]

Sheng WS, Hu S, Min X, Cabral GA, Lokensgard JR, Peterson PK. Synthetic cannabinoid WIN55,212–2 inhibits generation of inflammatory mediators by IL-1beta-stimulated human astrocytes. Glia. 2005; 49:211–219. [PubMed: 15390091]

Shi X, McGinty JF. Extracellular signal-regulated mitogen-activated protein kinase inhibitors decrease amphetamine-induced behavior and neuropeptide gene expression in the striatum. Neuroscience. 2006; 138:1289–1298. [PubMed: 16459022]

Sim LJ, Selley DE, Childers SR. *In vitro* autoradiography of receptor-activated G proteins in rat brain by agonist-stimulated guanylyl 5′-[gamma-[35S]thio]-triphosphate binding. Proc Natl Acad Sci USA. 1995; 92:7242–7246. [PubMed: 7638174]

Smith ME, Eng LF. Glial fibrillary acidic protein in chronic relapsing experimental allergic encephalomyelitis in SJL/J mice. J Neurosci Res. 1987; 18:203–208. [PubMed: 3682026]

Smith Y, Villalba R. Striatal and extrastriatal dopamine in the basal ganglia: an overview of its anatomical organization in normal and Parkinsonian brains. Mov Disord. 2008; 23(Suppl 3):S534–S547. [PubMed: 18781680]

van der Stelt M, DiMarzo V. The endocannabinoid system in the basal ganglia and in the mesolimbic reward system: implications for neurological and psychiatric disorders. Eur J Pharmacol. 2003; 480:133–150. [PubMed: 14623357]

Szabo B, Dorner L, Pfreundtner C, Norenberg W, Starke K. Inhibition of GABAergic inhibitory postsynaptic currents by cannabinoids in rat corpus striatum. Neuroscience. 1998; 85:395–403. [PubMed: 9622239]

Takeuchi Y, Miyamoto E, Fukunaga K. Activation of the rat dopamine D2 receptor promoter by mitogen-activated protein kinase and Ca^{2+}/calmodulin-dependent protein kinase II pathways. J Neurochem. 2002; 83:784–796. [PubMed: 12421350]

Tepper JM, Abercrombie ED, Bolam JP. Basal ganglia macrocircuits. Prog Brain Res. 2007; 160:3–7. [PubMed: 17499105]

Thanos PK, Gopez V, Delis F, Michaelides M, Grandy DK, Wang GJ, Kunos G, Volkow ND. Upregulation of cannabinoid type 1 receptors in dopamine D2 receptor knockout mice is reversed by chronic forced ethanol consumption. Alcohol Clin Exp Res. 2011; 35:19–27. [PubMed: 20958329]

Van Waes V, Beverley JA, Siman H, Tseng KY, Steiner H. CB1 Cannabinoid receptor expression in the striatum: association with corticostriatal circuits and developmental regulation. Front Pharmacol. 2012; 3:21. [PubMed: 22416230]

Warnault V, Houchi H, Barbier E, Pierrefiche O, Vilpoux C, Ledent C, Daoust M, Naassila M. The lack of CB1 receptors prevents neuroadapatations of both NMDA and GABA (A) receptors after chronic ethanol exposure. J Neurochem. 2007; 102:741–752. [PubMed: 17442049]

Xiao X, Li J, Samulski RJ. Production of high-titer recombinant adeno-associated virus vectors in the absence of helper adenovirus. J Virol. 1998; 72:2224–2232. [PubMed: 9499080]

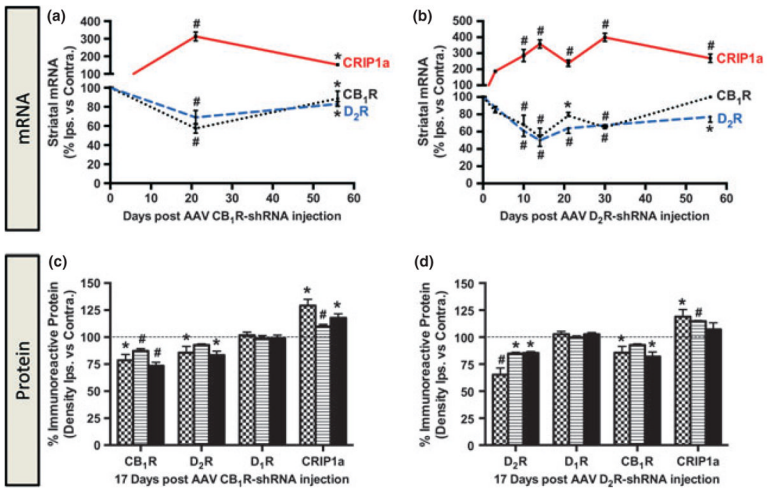

Fig. 1.

Effects of adeno-associated viral (AAV)-shRNA-mediated *in vivo* knockdown of CB_1R and D_2R on mRNA and protein levels. A mixture of three AAV-shRNAs specifically against CB_1R or D_2R was stereotaxically injected unilaterally into the dorsal striatum of adult male Sprague–Dawley rats. (a, b) qPCR analysis of shRNA-mediated knockdown of CB_1R (a) or D_2R (b) over a 56 day post-AAV injection period. Knockdown of CB_1Rs occurred concurrently with decreased D_2R mRNA levels and increased cannabinoid receptor interacting protein 1a (CRIP1a) mRNA levels (a). Knockdown of D_2R occurred concurrently with decreased CB_1R mRNA levels, and increased CRIP1a mRNA levels (b). (c, d) Immunohistochemical analysis of AAV-mediated knockdown of CB_1Rs (c) and D_2Rs (d). At 17 days post-AAV injection, 40 μm brain slices were obtained from the dorsal striatum (checkered bar), globus pallidus (striped bar), and entopeduncular nucleus (solid bar), and antibody staining was performed as described in the text. shRNA-mediated knockdown of CB_1Rs resulted in significantly decreased CB_1R protein levels in all three brain regions and significantly decreased D_2R levels in the dorsal striatum and entopeduncular nucleus (c). shRNA-mediated knockdown of D_2R resulted in significantly decreased D_2R protein levels in all three brain regions and significantly decreased CB_1R protein levels in the dorsal striatum and entopeduncular nucleus (d). Knockdown of CB_1R or D_2R significantly increased protein levels of CRIP1a in both the dorsal striatum and its outflow projections (c, d). Data are shown as mean ± SEM ($n = 5$; $^{*}p < 0.05$, $^{\#}p < 0.01$ paired Student's two-tailed *t*-test).

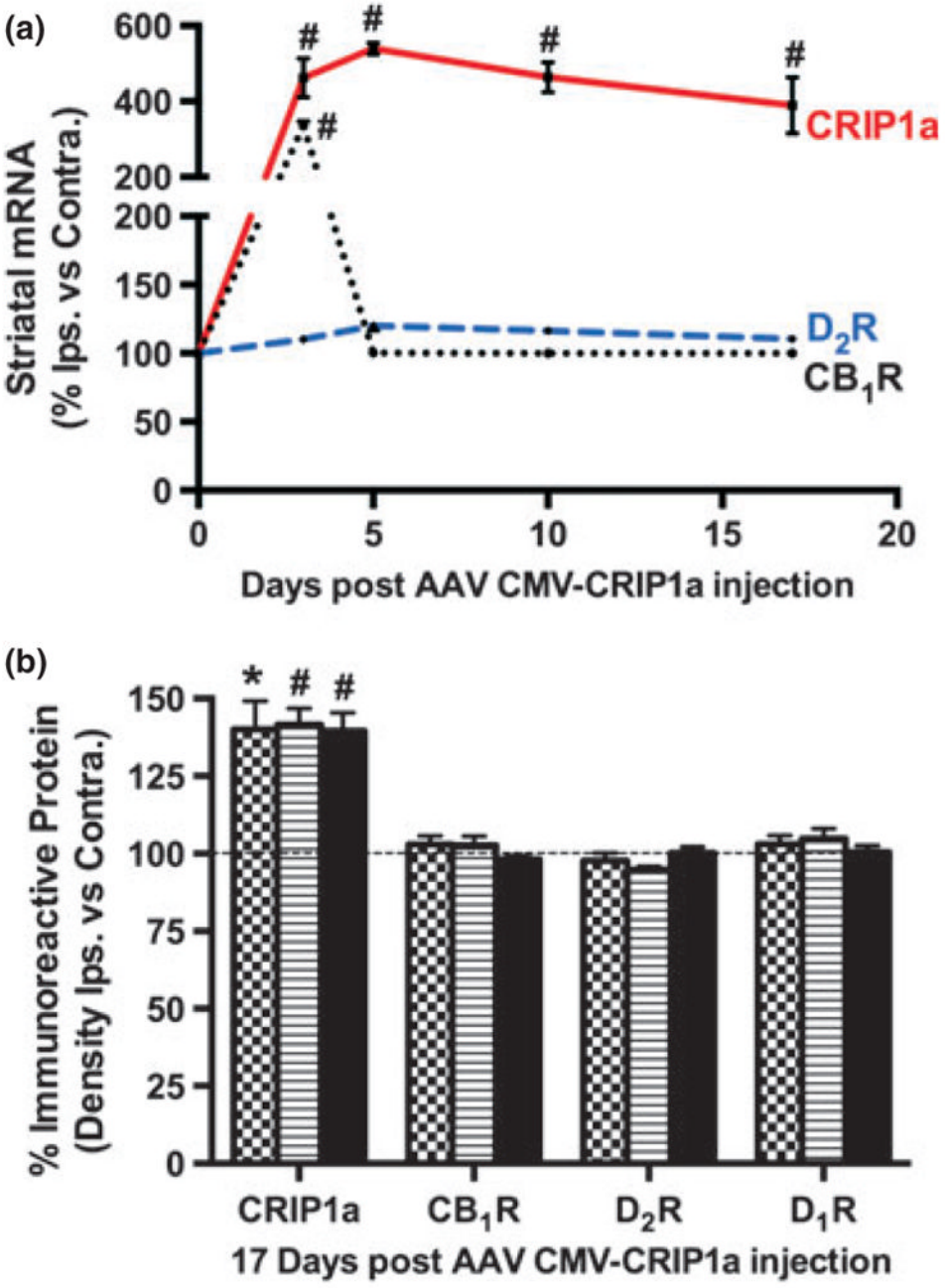

Fig. 2.

Effects of adeno-associated viral (AAV)-mediated over-expression of cannabinoid receptor interacting protein 1a (CRIP1a) in the rat striatum. (a, b) AAV-CRIP1a was unilaterally injected into rat dorsal striatum. (a) Animals were killed 3, 5, 10, and 17 days post-AAV-CRIP1a injection, and 2 × 2 mm brain punches were taken at the site of injection for qPCR analyses. Neuron-specific enolase (eno2) served as the reference standard and data were analyzed using the ΔΔCT method with the contralateral side serving as the control. AAV-CRIP1a treatment effects on CRIP1a, CB_1R, and D_2R transcript levels are shown as means ± SEM ($n = 5$, $^{*}p < 0.05$, $^{\#}p < 0.01$ paired Student's two-tailed *t*-test). (b) Immunohistochemical analysis from 40 μm coronal brain slices was performed at 17 days

post-AAV-CRIP1a treatment. Injection of AAV-CRIP1a significantly increased CRIP1a protein levels in the dorsal striatum (checkered bar) and the outflow projections to the globus pallidus (striped bar) and entopeduncular nucleus (solid bar), but did not significantly alter the immunoreactive protein levels of CB_1R, D_2R or D_1R. Data are shown as means ±SEM ($n = 5$; $^{*}p < 0.05$, $^{\#}p < 0.01$ paired Student's two-tailed t-test).

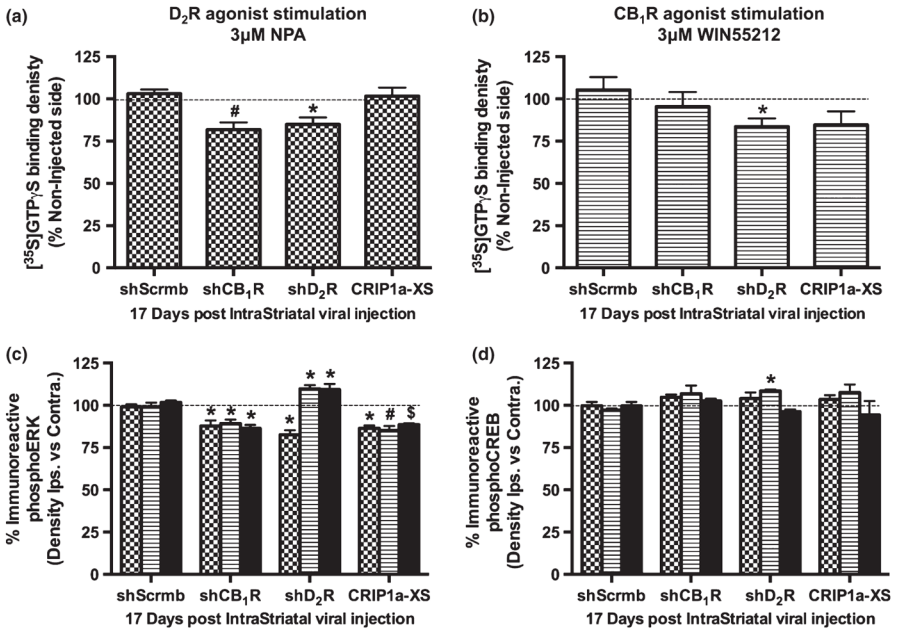

Fig. 3.

Influence of CB_1R or D_2R knockdown or CRIP1a over-expression on receptor-mediated G protein activation and downstream signaling. [^{35}S]GTPγS binding assays and immunohistochemical analyses for phosphoERK and phosphoCREB were performed on coronal brain slices from rats killed 17 days post-adeno-associated viral injection, as described in the text. (a, b) Striatal (checkered bars) or globus pallidus (striped bars) 20 μm brain slices were subjected to [^{35}S]GTPγS binding stimulated by the D_2R agonist *N*-propylnorapo-morphine (NPA) [3 μM] (a) or the CB_1R agonist WIN55212 [3 μM] (b). Data are reported as a percent of the contralateral control as 100% for each rat (means ± SEM, n = 4 rats) for [^{35}S]GTPγS binding (each with three technical replicates), and analyzed for differences between ipsilateral versus contralateral side by paired Student's two-tailed t-test ($^{*}p < 0.05$, $^{\#}p < 0.01$). Significant reductions in D_2R-stimulated G protein activity in the striatum were observed following knockdown of either the CB_1R or D_2R (a). A significant reduction in CB_1R-stimulated G protein activity in the globus pallidus was observed after knock-down of the D_2R receptor (b). (c, d) Immunohistochemical analyses of phosphoERK/total ERK and phosphoCREB/total CREB ratios following knockdown of CB_1R or D_2R, or over-expression of CRIP1a, were performed as described in the text. PhosphoERK and phosphoCREB protein levels were calculated as a ratio of phosphorylated to total ERK and CREB, respectively. No changes due to CB_1R or D_2R, or over-expression of CRIP1a were observed in total ERK or total CREB protein levels in any region (data not shown). Data are reported as a percent of the contralateral control as 100% for each rat (means ± SEM, n = 5 rats), and analyzed as the difference between ipsilateral versus contralateral side by paired Student's two-tailed t-test ($^{*}p < 0.05$, $^{\#}p < 0.01$, $^{\$}p < 0.001$). PhosphoERK/total ERK ratios were significantly reduced in both the striatum (checkered bar) and its outflow projections to the globus pallidus (striped bar) and entopeduncular nucleus (solid bar) following knockdown of CB_1R or over-expression of CRIP1a. PhosphoERK/total ERK ratios following knockdown of D_2R were changed in a bidirectional manner, with a significant decrease in the dorsal striatum and significant increases in the globus pallidus and entopeduncular nucleus (c). The phosphoCREB/total CREB ratio in the globus pallidus was significantly increased following D_2R knockdown (d).

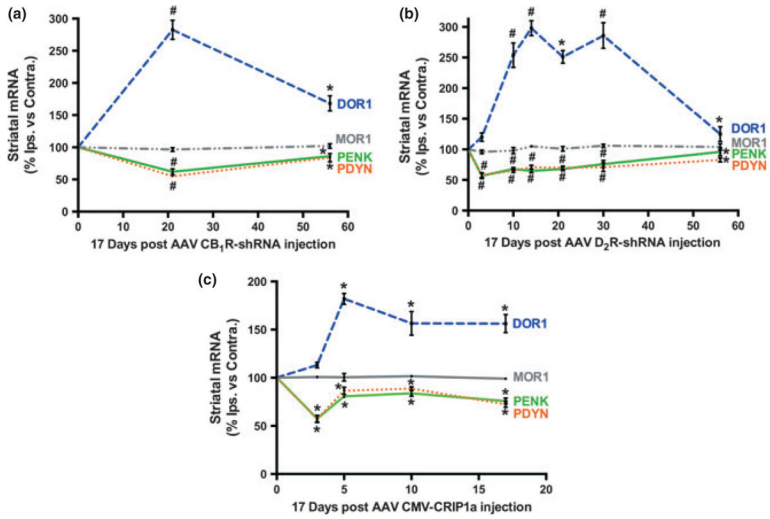

Fig. 4.

Knockdown of CB_1R and D_2R decreases striatal opioid peptide precursors and increases DOR1 transcript levels. Pro-enkephalin, pro-dynorphin, and opioid receptor mRNA levels were quantitated by qPCR on striatal brain punches collected 17 days after a single unilateral injection into the dorsal striatum of adeno-associated viral (AAV)-shCB_1R (a), AAV-shD_2R (b), or AAV over-expressing CRIP1a (c). Data were analyzed using the ΔΔCT method with the contralateral side as the control (100%), and are shown as means ± SEM (n = 5 rats). Differences between data from ipsilateral versus contralateral sides were statistically determined using a paired Student's two-tailed t-test (*$p < 0.05$, $^{\#}p < 0.01$). Significant decreases in pro-enkephalin and pro-dynorphin and increases in DOR1 transcripts were observed as indicated.

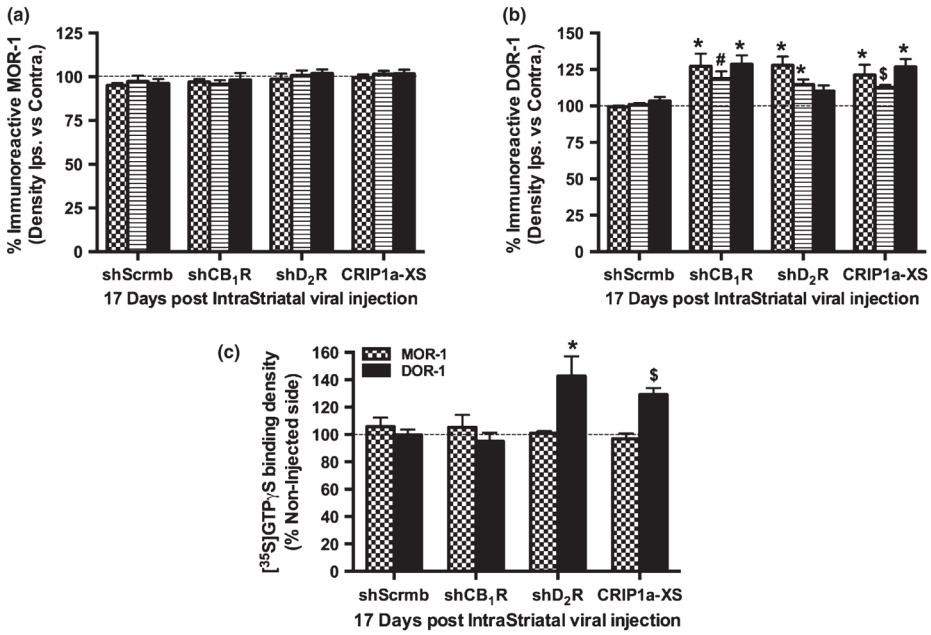

Fig. 5.

Opioid receptor levels and G protein activation following striatal knockdown of CB_1R or D_2R or over-expression of CRIP1a. Data are shown as immunoreactive MOR1 and DOR1 protein levels as a percent of the contralateral control value (100%) (means ± SEM, $n = 4$ rats) in the striatum (checkered bar), globus pallidus (striped bar) and entopeduncular nucleus (solid bar), and analyzed by a paired Student's two-tailed *t*-test ($^{*}p < 0.05$, $^{\#}p < 0.01$, $^{\$}p < 0.001$. (a) Knockdown of CB_1R or D_2R, and over-expression of CRIP1a in the dorsal striatum did not significantly alter MOR1 protein levels in any regions measured. (b) Knockdown of CB_1R or D_2R and over-expression of CRIP1a significantly increased DOR1 protein levels as indicated. (c) Striatal brain slices were subjected to [^{35}S] GTPγS binding stimulated by the MOR1 agonist D-Ala2, NMe-Phe4, Gly-ol5]-enkephalin [10 μM] (checkered bar) or the DOR1 agonist [D-Pen2, D-Pen5]-enkephalin [10 μM] (solid bar). Data are reported as a percent of the contralateral control side (100%) (means ± SEM, $n = 4$ rats) from [^{35}S]GTPγS binding measured in triplicates), and were analyzed using a paired Student's two-tailed *t*-test ($^{*}p < 0.05$, $^{\$}p < 0.001$).